RESONANT DIFFUSION IN PULSATED DEVICES*

Marcello Borromeo[a,b], Fabio Marchesoni[b,c]

[a]Dipartimento di Fisica, Università di Perugia, 06123 Perugia, Italy
[b]Istituto Nazionale di Fisica Nucleare, Sezione di Perugia, 06123 Perugia, Italy
[c]Dipartimento di Fisica, Università di Camerino, 62032 Camerino, Italy

(Received January 25, 2010)

Diffusion of an overdamped Brownian particle on a symmetric periodic substrate is investigated in the presence of pulsated perturbations of two kinds: *(i)* stepwise lateral displacements (flashing substrate), and *(ii)* instantaneous tilts (shot noise). Pulses are applied in either periodic or random sequences with assigned mean (bias) and average waiting time (time constant). At zero bias, the diffusion coefficient of the particle can be greatly enhanced by tuning the time constant. Such a diffusion resonance should not be mistaken for the excess diffusion peaks earlier reported for finite biases.

PACS numbers: 05.60.–k, 66.10.C–, 82.75.–z

1. Introduction

Brownian diffusion on a periodic substrate is often affected by *(i)* model A: instantaneous lateral shifts of the substrate (flashing substrate) and *(ii)* model B: external kicks corresponding to instantaneous substrate tilts (shot noise). Both jittering mechanisms have been advocated to model transport at the micro- and nanoscales [1,2]. Historically, models of type B were introduced first, originally, to interpret the output of classical electronic devices [3], and more recently, to engineer quantum devices subject to shot noise of either electronic [4] or photonic nature [5]. Prominent applications of model A include molecular motors at the cellular level [2,6], where flashing is caused by power strokes from the chemical energy source (like the hydrolysis of a single ATP molecule), tunable optical lattices for cold atoms [7], where substrate shifts are associated to degenerate atomic levels, and electromechanical sieves, *e.g.*, for the electrophoresis of DNA strands [8].

* Presented at the XXII Marian Smoluchowski Symposium on Statistical Physics, Zakopane, Poland, September 12–17, 2009.

In this paper we elaborate on the results first obtained in Ref. [9] by numerically simulating simple realizations of models A and B with particular attention to spatial diffusion.

2. Two models

Let x be the coordinate of an overdamped Brownian particle of unit mass diffusing on the cosine potential $V(x) = d[1 - \cos(2\pi x/L)]$. In the following we set, for convenience, $d = 1$ and $L = 2\pi$.

In model A the substrate shifts sidewise over time (see Fig. 1), *i.e.* $V(x) \to V[x - x_0(t)]$, where the drift $x_0(t)$ is either a squarewave,

$$x_0(t) = 2x_0 \sum_i (-1)^i \Theta(t - t_i) \tag{1}$$

(zero-bias drift), or a staircase,

$$x_0(t) = x_0 \sum_i \Theta(t - t_i) \tag{2}$$

(unidirectional drift). Here $\Theta(x)$ is a Heaviside step function, $\{t_i\}$ is an ordered sequence of the switch times with $i = 0, 1, 2 \ldots$ and $t \geq t_0$, and $x_0 > 0$ is the step length. We simulated both constant waiting times, $t_{i+1} - t_i \equiv \tau$ for

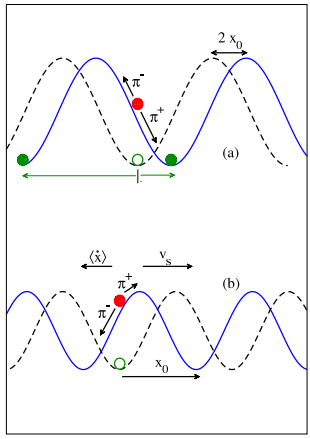

Fig. 1. (Color online) (a) Resonant diffusion. As the substrate switches between V_- (dashed curve) and V_+ (solid curve), in model A a particle initially at rest in a V_- well (empty circle) gets instantaneously activated (gray circle) and then diffuses either to the right or to the left (filled light gray circles) with probabilities $\pi_\pm$. (b) Negative mobility (model A). As the substrate advances to the right with average speed v_s, the activated particle (gray circle) may happen to preferably roll backwards with $\pi_- > \pi_+$.

any i (periodic sequence), and exponentially distributed waiting times, with time constant $\tau = \langle t_{i+1} - t_i \rangle$ (random sequence). In conclusion, model A is summarized by the Langevin Equation (LE) [10]

$$\dot{x} = -\sin[x - x_0(t)] + \xi(t)\,, \tag{3}$$

where $\xi(t)$ is a Gaussian zero-mean noise with autocorrelation function $\langle \xi(t)\xi(0) \rangle = 2kT\delta(t)$, which maintains the system at the equilibrium temperature T.

Model B is defined by imposing the spatial variable transformation $x \to x - x_0(t)$ on the corresponding model A. Accordingly, the LE (3) becomes

$$\dot{y} = -\sin y + F_{\rm S}(t) + \xi(t)\,, \tag{4}$$

where $F_{\rm S}(t) \equiv -\dot{x}_0(t)$ can be regarded as a shot noise acting upon the Brownian particle of coordinate y, diffusing in the *static* cosine potential $V(y)$. Correspondingly, the zero-bias, (1), and unidirectional drift, (2), are mapped into a sequence of δ-like pulses with alternate,

$$F_{\rm S}(t) = -2x_0 \sum_i (-1)^i \delta(t - t_i)\,, \tag{5}$$

or equal signs,

$$F_{\rm S}(t) = -x_0 \sum_i \delta(t - t_i)\,. \tag{6}$$

Moreover, due to the linear nature of the transformation $x \to y$, models A and B have the same diffusion coefficient D [10,11]. For numerical purposes we computed D for model A, *i.e.*, $D \equiv \lim_{t\to\infty}[\langle x^2(t) \rangle - \langle x(t) \rangle^2]/2t$.

3. Outline

In the current literature [3], the unidirectional drifts of model A and the unidirectional shot noises of model B are often characterized in terms of their time averages, respectively, the net drift velocity of the substrate, $v_{\rm s} = x_0/\tau$, and the net driving force, $f_{\rm s} = -x_0/\tau$, felt by the particle. In fact, this approach typically holds good for macroscopic devices, where τ is negligible with respect to the device response times. On the contrary, we show below that the interplay of time-pulsated perturbations and spatial periodicity may strongly affect particle transport in a small device. By tuning τ at *constant* bias, $v_{\rm s}$ or $f_{\rm s}$, we observed (a) Model A: *negative mobility* dips with $\mu_{\rm A} \equiv \langle \dot{x} \rangle / v_{\rm s} < 0$, indicating particles that drift with average velocity opposite to the substrate drift; (b) Model B: *excess mobility* peaks with $\mu_{\rm B} \equiv \langle \dot{y} \rangle / f_{\rm s} > 1$, implying that, for an appropriate τ, shot noise can push particles faster than in the absence of substrate barriers (in which case $\mu_{\rm B} = 1$

[12]), and correspondingly, (c) *excess diffusion* peaks with $D > kT$, which appear to anticipate both the dips, (a), and the peaks, (b), of the mobility curves. [In our notation the diffusion coefficient of a free Brownian particle (*i.e.*, for $V \equiv 0$) is kT]. Finally, in both models, for *zero bias* ($v_s = f_s = 0$) and an appropriate τ interval, we observed (d) a remarkable *resonant diffusion* effect, also with $D > kT$. Properties (a)–(d) can be regarded as manifestations of a *resonant transport* mechanism controlled by the time constant of the pulse sequence.

4. Zero bias: Resonant diffusion

We start now analyzing the results of our simulations for the processes (1) and (2) at *zero-bias*. In Fig. 2 we display D/kT *versus* τ at different temperatures; the pulse sequences are periodic in panel (a) and random in panel (b). The resonant nature of the curves $D(\tau)$ is apparent in both panels, although more prominent for periodic sequences.

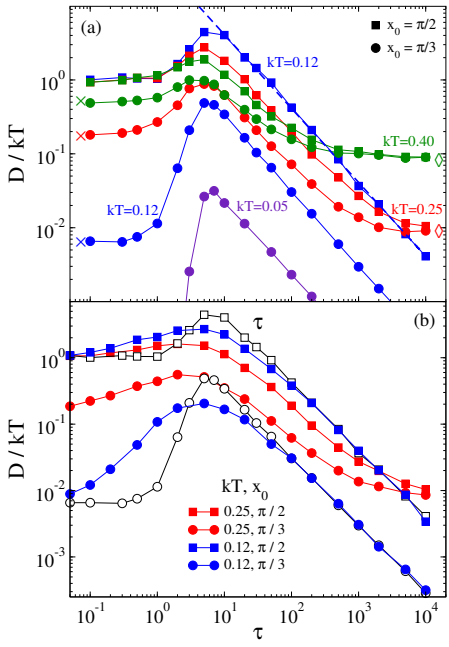

Fig. 2. (Color online) (a) Resonant diffusion D/kT *versus* τ for an unbiased pulsated substrate (the same for model A and B). The squarewave $x_0(t)$ is periodic in (a) and random in (b). The simulation parameters kT and x_0 are reported in the legend. Crosses and lozenges in (a) are the relevant analytical predictions for $\tau \to 0$ and $\tau \to \infty$, respectively (see text). The dashed line in (a) is the optimal diffusion law (7) for $x_0 = \pi/2$. Two data sets from (a) (blue symbols) have been reported in (b) (empty symbols) for reader's convenience.

We interpret such an effect as a new instance of the so-called resonant activation phenomenon, originally demonstrated in bistable systems [13]. For exceedingly large τ, say, $\tau \to \infty$, Brownian diffusion achieves its asymptotic regime, $\langle x^2(t)\rangle - \langle x(t)\rangle^2 = 2D(\infty)t$, irrespective of the applied perturbation $x_0(t)$. The coefficient $D(\infty)$ thus coincides with the diffusion coefficient in the static, unbiased cosine potential $V(x)$, namely, $D(\infty) = kT\mu(d)$, where $\mu(d) = [I_0(d/kT)]^2$ is the relevant mobility, expressed in terms of the modified Bessel function $I_0(x)$ [12]. In the opposite limit, $\tau \to 0$, the diffusion process takes place in the effective potential $\overline{V}(x)$, obtained by time averaging either the sidewise switches $x_0(t)$ (model A) or the kicks $F_S(t)$ (model B). Upon implementing the vibrational mechanics scheme utilized in Refs. [14], one concludes that $\overline{V}(x)$ is still a cosine potential, but with rescaled amplitude $d \to d\cos x_0$. As a consequence, for vanishingly small τ, $D(0) = kT\mu(d\cos x_0)$. Our analytical estimates for $D(0)$ and $D(\infty)$ are also reported in Fig. 2 (a). Note that, at variance with $D(\infty)$, $D(0)$ sharply depends on x_0. In particular, $D(0) \geq D(\infty)$ for any x_0 and $D(0) = kT$ (free diffusion) for $x_0 = \pi/2$. Moreover, the unbiased LE (3) and (4) are invariant for $x_0 \to x_0 + \pi$, as explicitly shown in Fig. 3.

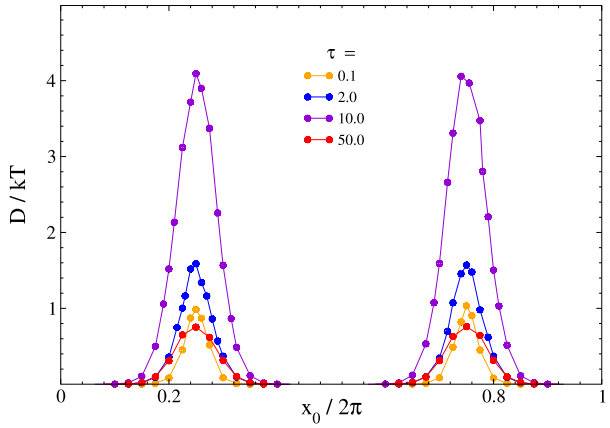

Fig. 3. (Color online) Diffusion coefficient D *versus* x_0 for $kT = 0.12$, vanishing bias and different τ (model A). The D peaks are symmetric and periodic with period $x_0 = \pi$.

The $D(\tau)$ curves bridge the two limits $D(0)$ and $D(\infty)$ by going through a broad *resonance* peak. Such excess diffusion peaks can be explained also by means of a simple argument. Let us consider, for instance, a substrate switch from $V_-(x) \equiv V(x+x_0)$ to $V_+(x) \equiv V(x-x_0)$ in model A. A particle initially sitting at a minimum of $V_-(x)$, now finds itself kicked a distance $2x_0$ to the left from the corresponding minimum of the shifted $V_+(x)$, as sketched in Fig. 1 (a). In the overdamped regime, one can then introduce the *splitting*

probabilities for the particle to relax toward the nearest $V_+(x)$ minimum to either the right, $\pi_+(x_0)$, or the left, $\pi_-(x_0) = 1 - \pi_+(x_0)$. The continuous particle dynamics (3) is thus mapped into a discrete random-walker process with [3]

$$D(\tau) = \frac{L^2}{2\tau}\,\pi_+(x_0)[1 - \pi_+(x_0)]\,, \tag{7}$$

where $L = 2\pi$ and analytical expressions for $\pi_+(x_0)$ are derived in Sec. 9.1 of Ref. [3]. This law fits well the decaying branch of our $D(\tau)$ curves [15]. In Fig. 2 (a) an explicit comparison is shown for the optimal choice $x_0 = \pi/2$, corresponding to $\pi_\pm(x_0) = 1/2$. Note that the resonant D peaks get sharper and sharper as one lowers T.

Finally, as to be expected, the resonant D peak occurs at around the smallest time constant, $\tau_{\rm R}$, for which the optimal diffusion law (7) applies. Indeed, the random walker scheme leading to that law assumes implicitly that τ is no smaller than the relaxation time of a kicked particle towards the nearest potential minimum, so that, in our notation, $\tau_{\rm R} \sim L/d = 2\pi$ [12].

The phenomenon of resonant diffusion can be related to the observation that the stochastic response of a Brownian particle gets hypersensitive to an external drive, if the particle is subjected to an additional dichotomic noise that drives it across the unstable fixed points of the underlying dynamics [16]. Indeed, as mentioned above, in the zero bias limit the particle mobility is proportional to its diffusion coefficient. However, the resonant diffusion effect of Figs. 2 and 3 should not be mistaken for the damped D oscillations induced by periodic bimodal [17] or trimodal additive symmetric forces [18] applied to a Brownian particle in a periodic potential. In Ref. [18] D/kT oscillations are reported for constant tilt amplitudes, F_0, as a function of the tilting time, $t_{\rm t}$. In the notation of model B, (4), such finite-time tilting pulses are replaced by instantaneous kicks of strength $x_0 = F_0 t_{\rm t}$. As a consequence, the damped D oscillations reported in Ref. [18] must be regarded as the counterpart of the periodic oscillations of D *versus* x_0 displayed in Fig. 3 (damping being due to the finiteness of $t_{\rm t}$). In this case, as well as in Ref. [17], we are in the presence of a commensuration effect between pulse strength x_0 and spatial periodicity of the substrate, whereas resonant diffusion is rather controlled by the waiting time between consecutive kicks.

5. Zero bias: asymmetric sequences

Asymmetric variations of the zero-bias sequences (1) and (5) were also simulated by assuming different average waiting times of $x_0(t)$ in the $\pm$ state, $\tau_\pm$, with

$$\overline{\tau} = \tfrac{1}{2}\,(\tau_+ + \tau_-) \tag{8}$$

and

$$R = \tau_+/\tau_- \,. \tag{9}$$

The asymmetric character of the pulsated sequence becomes apparent as R decreases, with $0 < R \leq 1$. The corresponding plots of D *versus* $\overline{\tau}$ as displayed in Fig. 4 for *periodic* sequences with different R.

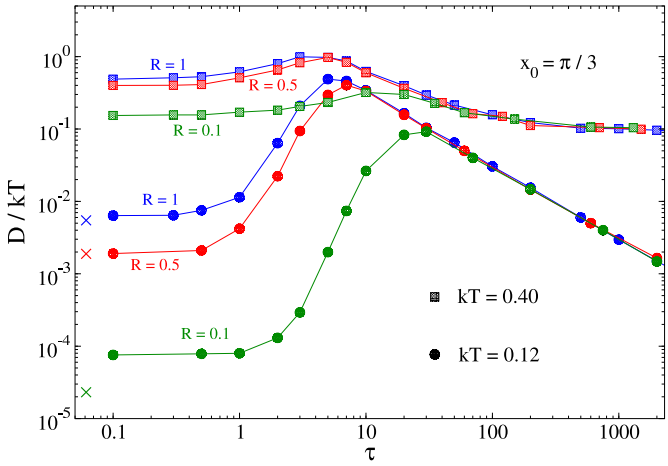

Fig. 4. (Color online) (a) Resonant diffusion D/kT *versus* $\overline{\tau}$ for pulsated sequences with different asymmetry ratios R. The squarewave $x_0(t)$ is periodic with $\tau_\pm$ expressed in terms of $\overline{\tau}$ and R as in Eqs. (8) and (9). The simulation parameters kT and x_0 are reported in the legend. Crosses are the relevant vibrational mechanical predictions for $\overline{\tau} \to 0$ at $kT = 0.12$.

As expected, for $\overline{\tau} \to \infty$ the spatial diffusion grows insensitive to the pulsated perturbation, whereas for $\overline{\tau} \to 0$ the coefficient D gets strongly suppressed at small R. As for the symmetric case, $R = 1$, here too vibrational mechanics provides an analytical approximation for the amplitude of the effective potential $\overline{V}(x)$, *i.e.*,

$$d \to d\sqrt{1 - \frac{4R}{(1+R)^2}\sin^2 x_0}\,.$$

The corresponding values of $D(0)$, marked by a cross in Fig. 4, closely agree with our simulation results for $\overline{\tau} \to 0$. In conclusion, asymmetry tends to suppress resonant diffusion and to shift the diffusion peak to higher $\overline{\tau}$. This statement applies to random sequences, as well.

6. Finite bias: mobility oscillations and diffusion peaks

We investigate now models A and B under the action of a *unidirectional* pulse sequence (2). In model A, the substrate drifts to the right with average speed $v_s = x_0/\tau$, while in model B, the shot noise has negative mean, $f_s = -v_s$. Owing to the transformation, $y = x - x_0(t)$, connecting the two processes (3) and (4), the relevant mobility functions, $\mu_{A,B}$, obey the identity $\mu_A = 1 - \mu_B$ (whereas, as mentioned above, D is the same). This means that excess peaks of μ_B correspond to negative dips of μ_A. Of course, in the absence of a substrate $\mu_B = 1$ and $\mu_A = 0$ for any choice of $x_0(t)$ [12].

In Fig. 5 we illustrate the bias dependence of D for different step lengths x_0. The process (3) is symmetric under the transformation $x_0 \to -x_0$ (mirror reflection) and $x_0 \to x_0 + L$, with $L = 2\pi$ (step-substrate commensuration), as apparent on displaying our data *versus* the reduced bias $[x_0]/\tau$, with $[x_0] = x_0 \mod(2\pi)$. All diffusion curves peak for $[x_0]/\tau$ in the vicinity of the substrate depinning threshold d (namely, the least force required to drag a noiseless particle over a substrate barrier). Being a threshold effect [19], diffusion enhancement peaks are associated to steps in the mobility curves (also shown in Fig. 5). (In the notation of model B the connection with the earlier literature is more apparent.) However, decreasing $[x_0]/\tau$

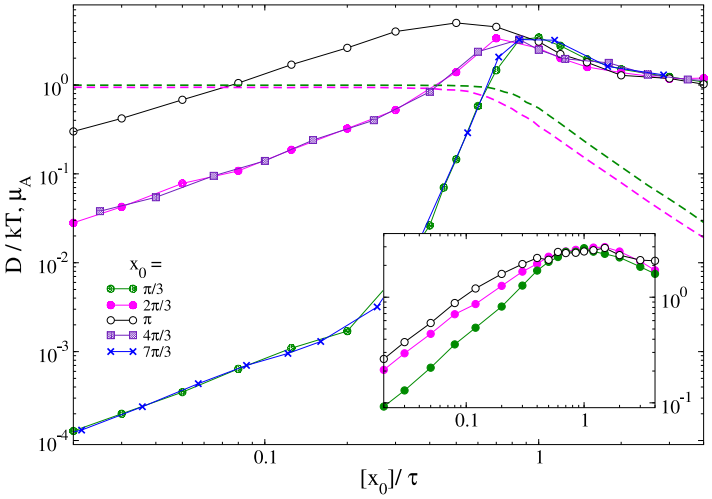

Fig. 5. (Color online) Transport on a sinusoidal substrate traveling with velocity $v_s = [x_0]/\tau$, where $[x_0] = x_0 \mod(2\pi)$ (model A). The unidirectional step sequence is periodic in the main panel and random in the inset; x_0 was chosen to demonstrate the symmetry and under transformations $x_0 \to -x_0$ and $x_0 \to x_0 + 2\pi$ (see text). The relative diffusion coefficient is represented by circles and the mobility $\mu_A = \langle \dot{x} \rangle / v_s$ by dashed curves. For $x_0 = \pi$ the mobility is zero within our numerical accuracy. The color code in the inset is the same as in the main panel.

at constant x_0 means increasing τ, so that, at variance with the setup of Refs. [19], the pulsated nature of the drive now starts playing a role. Indeed, the linear tails, $D \propto [x_0]/\tau$, of Fig. 5 correspond to the linearly decaying branches (7) displayed in Fig. 2 (a). For $[x_0]/\tau \to 0$ (not shown) all numerical curves eventually approach the asymptotic limit $D(\infty)$ for the zero-bias case. Finally, we stress that all the above applies both to periodic (main panel) and random pulse sequences (inset), alike.

To illustrate the role of the drift time constant, in Fig. 6 we display our data for μ_B [panel (a)] and D [panel (b)] *versus* τ at constant bias f_s. The curves $\mu_B(\tau)$ exhibit damped oscillations with maxima exceeding unity. This result may sound surprising as it implies that, for appropriate τ, shot noise can push particles faster than in the absence of a substrate (in which case $\mu_B = 1$ [12]). However, when kicked by a δ-like pulse with strength $x_0 \sim \pi$, a particle initially at rest may reach the top of one confining barrier,

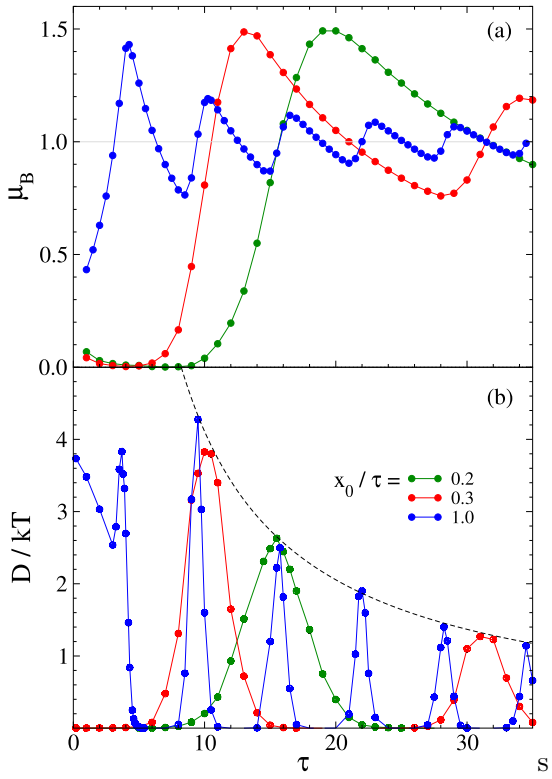

Fig. 6. (Color online) Transport enhancement induced by a period pulse sequence with fixed bias $v_s = x_0/\tau$ (model A) and varying τ. The mobility drops in (a) correspond to sharp diffusion peaks in (b). The dashed curve in (b) locates the maxima $\pi^2/2\tau$ of the resonant D.

either to the left or to the right, and then cross into the neighboring well, thus advancing by up to twice the distance of a free particle; hence the excess mobility peaks $\mu_{\rm B} > 1$. This mechanism applies for x_0 close to $(2m+1)\pi$, $m = 0, 1, 2\ldots$, so that excess mobility peaks are expected for $\tau \simeq (2m+1)\pi/|f_{\rm s}|$, in agreement with our numerics. Extending this argument to model A also explains the negative $\mu_{\rm A}$ dips reported in Ref. [15].

In Fig. 6 (b) we displayed the corresponding curves $D(\tau)$ for the same τ range as in Fig. 6 (a): The correlation between D peaks and $\mu_{\rm A}$ drops is apparent. Most remarkably, the peaks for relatively large τ fall on the envelope curve $L^2/8\tau$, with $L = 2\pi$, as one guesses by inspecting the linear D tails in Fig. 5. Such tails shift upwards on increasing x_0 from $2m\pi$ to $(2m+1)\pi$, so that the diffusion maxima in Fig. 6 (b) must occur for $x_0 = (2m+1)\pi$. The envelope curve drawn there is simply the optimal diffusion law (7) with $\pi_+[(2m+1)\pi] = 1/2$.

7. Conclusions

In summary, a particle diffusing on a pulsated periodic substrate, for appropriate combinations of the amplitude and frequency of the pulses, can synchronize its dynamics with the pulse sequence, which allows an effective control of the particle delivery (*i.e.*, of both its speed and dispersion) [20]. When utilized in particle separation, such delivery control technique can be exploited to increase the separation speed and selectivity. Preliminary estimates indicate that ideal experimental set-ups to demonstrate the resonant diffusion mechanisms introduced here, are the optical potentials for colloidal particles investigated in Refs. [21, 22].

REFERENCES

[1] P. Hänggi, F. Marchesoni, F. Nori, *Ann. Phys.* **14**, 51 (2005); P. Hänggi, F. Marchesoni, *Rev. Mod. Phys.* **81**, 387 (2009).

[2] R.D. Astumian, P. Hänggi, *Phys. Today* **55**, 33 (2002).

[3] C.W. Gardiner, *Handbook of Stochastic Methods*, Springer, Berlin 1996.

[4] Y.M. Blanter, M. Büttiker, *Phys. Rep.* **336**, 1 (2000).

[5] C.H. Henry, R.E. Kazarinov, *Rev. Mod. Phys.* **68**, 801 (1996).

[6] Y.-D. Chen, *Phys. Rev. Lett.* **79**, 3117 (1997).

[7] L.P. Faucheux, L.S. Bourdieu, P.D. Kaplan, A.J. Libchaber, *Phys. Rev. Lett.* **74**, 1504 (1995); C. Mennerat-Robilliard, *et al.*, *Phys. Rev. Lett.* **82**, 851 (1999); R. Gommers, S. Bergamini, F. Renzoni, *Phys. Rev. Lett.* **95**, 073003 (2005); R. Gommers, S. Denisov, F. Renzoni, *Phys. Rev. Lett.* **96**, 240604 (2006).

[8] A. Ajdari, J. Prost, *C. R. Acad. Sci. Paris (Ser. II)* **315**, 1635 (1992); T.A.J. Duke, R.H. Austin, *Phys. Rev. Lett.* **80**, 1552 (1998); D. Ertas, *Phys. Rev. Lett.* **80**, 1548 (1998).

[9] M. Borromeo, F. Marchesoni, *Phys. Rev.* **E78**, 051125 (2008).

[10] M. Borromeo, F. Marchesoni, *Phys. Lett.* **A249**, 199 (1998).

[11] C. Van den Broeck, *Europhys. Lett.* **46**, 1 (1999).

[12] H. Risken, *The Fokker–Planck Equation*, Springer, Berlin 1984, Ch. 11.

[13] C.R. Doering, J.C. Gadoua, *Phys. Rev. Lett.* **69**, 2318 (1992); M. Bier, R.D. Astumian, *Phys. Rev. Lett.* **71**, 1649 (1993); M. Marchi, F. Marchesoni, L. Gammaitoni, E. Menichella-Saetta, S. Santucci, *Phys. Rev.* **E54**, 3479 (1996).

[14] M. Borromeo, F. Marchesoni, *Europhys. Lett.* **72**, 362 (2005); M. Borromeo, F. Marchesoni, *Phys. Rev.* **E73**, 016142 (2006).

[15] M. Borromeo, F. Marchesoni, *Phys. Rev.* **E78**, 051125 (2008).

[16] I. Bena, C. Van den Broeck, R. Kawai, K. Lindenberg, *Phys. Rev.* **E66**, 045603(R) (2002).

[17] H. Gang, A. Daffertshofer, H. Haken, *Phys. Rev. Lett.* **76**, 4874 (1996).

[18] M. Schreier, P. Reimann, P. Hänggi, E. Pollak, *Europhys. Lett.* **44**, 416 (1998).

[19] G. Costantini, F. Marchesoni, *Europhys. Lett.* **48**, 491 (1999); P. Reimann, C. Van den Broeck, H. Linke, P. Hänggi, J.M. Rubi, A. Pérez-Madrid, *Phys. Rev. Lett.* **87**, 010602 (2001); B. Lindner, M. Kostur, L. Schimansky-Geier, *Fluct. Noise Lett.* **1**, R25 (2001); D. Reguera, G. Schmid, P.S. Burada, J.M. Rubi, P. Reimann, P. Hänggi, *Phys. Rev. Lett.* **96**, 130603 (2006).

[20] L. Machura, M. Kostur, P. Talkner, J. Łuczka, F. Marchesoni, P. Hänggi, *Phys. Rev.* **E70**, 061105 (2004).

[21] Y. Roichman, V. Wong, D.G. Grier, *Phys. Rev.* **E75**, 011407 (2007).

[22] W. Mu, Z. Li, L. Luan, G.C. Spalding, G. Wang, J.B. Ketterson, *J. Opt. Soc. Am.* **B25**, 763 (2008).